Macromolecules

ARTICLE

pubs.acs.org/Macromolecules

Smart Chitosan-Based Stimuli-Responsive Nanocarriers for the Controlled Delivery of Hydrophobic Pharmaceuticals

Daoben Hua,*[,†,‡] Jianlin Jiang,[†] Liangju Kuang,[‡] Jing Jiang,[†] Wan Zheng,[‡] and Hongjun Liang*[,‡]

[†]Key Laboratory of Organic Synthesis of Jiangsu Province, College of Chemistry, Chemical Engineering and Materials Science, Soochow University, Suzhou 215123, P. R. China

[‡]Department of Metallurgical and Materials Engineering, Colorado School of Mines, Golden, Colorado 80401, United States

Supporting Information

ABSTRACT: We report here a green chemistry method to conjugate hydrophobic payloads (Lilial as a prototype) highly efficiently (35.8 wt %) with (1→4)-2-amino-2-deoxy-β-D-glucan (i.e., chitosan) via Schiff base bond formation in an ionic liquid, which renders chitosan easily dissolvable in common organic solvents and amenable to further functional modifications. As an example, thermoresponsive poly(*N*-isopropylacrylamide) was grafted to the chitosan−Lilial conjugate. The graft copolymer self-assembled in water at neutral pH into core−shell nanocarriers with a favorable size distribution ($d \sim 142 \pm 60$ nm) for intravenous administration. Under conditions of enhanced temperature and acidity ($T = 37$ °C, pH = 4.5) mimicking endosomal or lysosomal uptake, the nanocarriers fell apart and formed reversed micelles with greatly reduced sizes ($d \sim 8 \pm 3$ nm) favoring clearance by renal filtration, and 70% Lilial molecules were liberated within 30 h through hydrolytic cleavage of the exposed Schiff base conjugation. This smart stimuli-responsive drug release profile reveals a viable approach in the development of chitosan-based nanocarriers for intravenous administration of hydrophobic pharmaceuticals.

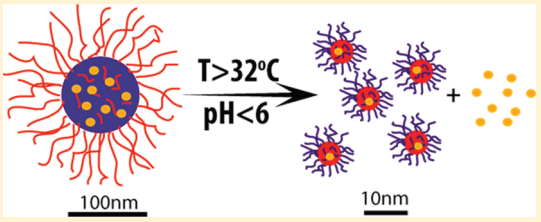

1. INTRODUCTION

Controlled delivery of insoluble therapeutic agents in a dose-, time-, and disease-specific manner across aqueous physiological pathways remains an outstanding challenge. This challenge is particularly troublesome in the fighting of cancers since most chemotherapy agents proposed for the treatment of localized and metastasized cancers are fairly hydrophobic with narrow therapeutic indices.[1,2] Polymer conjugates emerge as a potent approach, where hydrophobic pharmaceuticals are covalently bonded with chemically versatile polymer chains to obtain favorable pharmacokinetics.[3−10] To develop a viable polymer conjugate system with promising potential for efficaciously treating diseases with minimum side effects from the drug's toxicity and eventually passing clinical trials, at least four material-specific characteristics are needed:[4−13] (i) the polymer itself must be inherently biocompatible; (ii) it must also be amenable to industry scale production and cost-effective pharmaceutical formulation; (iii) the polymer−drug conjugates must have the right range of sizes (10−200 nm) to survive both rapid renal filtration and elimination by the reticuloendothelial system (RES) during intravenous administration, which is crucial to optimize their chance to reach the disease sites; and (iv) the polymer−drug conjugation must be strong enough to yield zero premature drug release in the storage or transit stages but labile for deterioration after cellular uptake to liberate the active payloads in a controlled manner. The polymer chains must be either small enough or biodegradable to become small enough to be cleared by renal filtration or other bioabsorbable mechanisms after the drugs are released.

We report here a green chemistry approach to design chitosan (CS)-based polymer−drug conjugates that aim to achieve all of the above-mentioned characteristics. CS is deacetylated chitin, a natural polysaccharide with enormous availability in the biosphere.[14,15] It is widely regarded as a nontoxic, nonimmunogenic, biocompatible polymer according to most *in vitro* and *in vivo* studies and is biodegradable and bioabsorbable by various enzymes in the human body.[14−18] Despite these inherent advantages, adapting CS for drug delivery, particularly for the delivery of hydrophobic therapeutic agents, has been greatly hampered by its intractability.

Owing to its semicrystalline nature and multiple H-bond-forming groups, the cohesive energy density of CS is very high (solubility parameter $\delta = 41$ J$^{1/2}$/cm$^{3/2}$).[19] As a result, CS is insoluble in water (when pH > 6.2) and all common organic solvents.[14,15] Interestingly, the pK_a of the $-NH_2$ group on CS is 6.3, and CS is dissolvable by salt formation in acidic aqueous solution up to pH ~6.2.[14,15] This property has been exploited extensively for developing CS-based drug delivery systems. For instance, CS and DNA coacervated complexes have been widely studied for gene delivery.[8,20] Micro- or nanostructured CS-based

Received: November 10, 2010
Revised: January 18, 2011
Published: February 04, 2011

Scheme 1. Synthetic Route for Obtaining PNIPAm−CS−Lilial Conjugated Copolymer

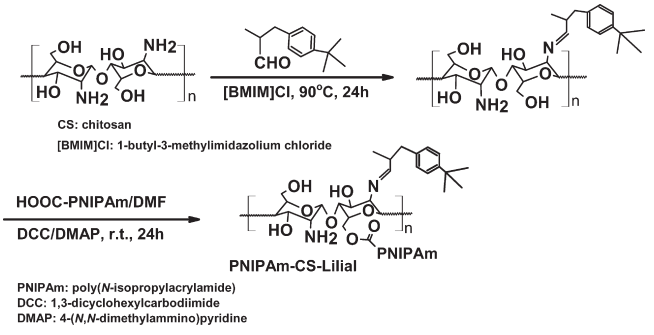

carriers obtained by ionic gelation,[21] reverse-micelle formation,[22] microemulsion,[23] and other methods[17] using acid solution-dissolved CS have also been enthusiastically pursued, where the water-soluble pharmaceutical payloads are physically encapsulated by either incorporation during the carrier formation or incubation afterward. However, limited approaches exist to improve the solubility of CS in organic solvents, which makes it extremely difficult for the chemical conjugation of CS with hydrophobic drug molecules or regioselective modification of CS to optimize the system design. One often-used approach is N-phthaloylation,[24] but this multiple-step process is a tedious operation that jeopardizes the integrity of CS chain structure.[25]

We consider the pH-dependent dissolution−coagulation transition of CS in aqueous solution to be a unique advantage for CS-based nanomedicine design, especially for drug-delivery system design since endosomal or lysosomal uptake is a gradually acidified compartmentalization process (pH ∼6.5−4).[4−11] Within this compass, the $-NH_2$ groups on CS can be conveniently employed to form Schiff base bond conjugations with hydrophobic drug molecules bearing an aldehyde group, which not only emancipates $-NH_2$ groups from the H-bonding network to improve CS solubility but also helps achieve a controlled drug release profile since the Schiff base bond is stable at neutral pH (e.g., during storage or transit) but is progressively hydrolyzed to break apart when pH drops below 6 (e.g., after endosomal or lysosomal uptake).[26] We choose 3-(4-*tert*-butylphenyl)isobutyraldehyde (i.e., Lilial) as a prototypical hydrophobic drug molecule; it has been frequently used in cosmetics and was recently discovered to have estrogenic activity in human breast cancer cells.[27] We adapt a green chemistry approach[28] to conjugate Lilial with CS in an ionic liquid (1-butyl-3-methylimidazolium chloride, [BMIM]Cl) identified as a good solvent for CS (Scheme 1).[29] The aldehyde group can be introduced to many chemotherapy drugs by a convenient functionalization step. For instance, typical anticancer agents such as paclitaxel, camptothecin, doxorubicin, and docetaxel all possess hydroxyl groups that can be used to graft with an aldehyde moiety. Aldehyde-derivatized chromones (a promising antiviral and anticancer agent[30]) have indeed been reported and demonstrated efficient inhibition to tumor cell proliferation.[31] We further demonstrate here as an example that well-defined poly(*N*-isopropylacrylamide) (PNIPAm) (number-average molecular weight, M_n = 8400 g/mol; molecular weight distribution, M_w/M_n = 1.21), a thermoresponsive polymer that has a hydrophilic coils−hydrophobic globules transition around 32 °C,[32,33] can be grafted to CS with controlled graft density by a facile esterification process (Scheme 1). We study here the self-assembly behavior of the PNIPAm−CS−Lilial conjugate as well as the stimuli-responsive release of Lilial as a function of temperature and pH. The results we obtained have direct relevance to the intravenous administration of hydrophobic pharmaceuticals using natural polymers and point out a promising direction to design a CS-based nanocarrier platform for the delivery of chemotherapy agents.

2. EXPERIMENTAL SECTION

Materials and Reagents. CS (degree of deacetylation = 95.2%, M_n = 50 000 Da) was purchased from Qingdao Haoda Biochemical Co., Shandong, China. NIPAM was purchased from J&K Chemical Co. Ltd. and was purified by recrystallization in benzene/*n*-hexane (3:1) before use. *S*-1-Dodecyl-*S*′-(α,α′-dimethyl-α″-acetic acid)trithiocarbonate (DATC) was synthesized according to the related reference.[34] [BMIM]Cl was synthesized by the modified method according to the literature (Supporting Information).[35] Carboxyl-terminated PNIPAM (M_n = 8400 g/mol, M_w/M_n = 1.21) was synthesized by reversible addition−fragmentation chain transfer (RAFT) polymerization according to the literature method (Supporting Information).[36] Lilial was purchased from Tokyo Chemical Industry (TCI) and used as received. 1,3-Dicyclohexylcarbodiimide (DCC, 99%), and 4-(*N*,*N*-dimethylamino)-pyridine (DMAP, 99%) were purchased from Alfa Aesar China (Tianjin) Co., Ltd. All other chemical reagents were of analytical grade and used without further purification.

Characterization Methods. ^{1}H nuclear magnetic resonance (^{1}H NMR) spectra were obtained on a Varian INVOA-400 instrument working at 300 MHz; Fourier transform infrared (FT-IR) spectra were recorded on a Varian-1000 spectrometer. The samples were ground with KBr crystals, and the mixture was then pressed into a pellet for IR measurement; The *Z*-average size distribution of the micelles were measured by dynamic light scattering (DLS) using a Malvern Zetasizer. The molecular weights and polydispersities of the homopolymers were determined with a Waters 1515 gel permeation chromatograph (GPC) equipped with refractive index detector, using HR1, HR3, and HR4 columns with molecular weight range 100−500 000 calibrated with polystyrene standard samples. THF was used as the eluent at a flow rate of 1.0 mL min^{-1} operated at 30 °C. Transmission electron microscopy (TEM) images were taken with a FEI Tecnai G20 electron microscope with an accelerating voltage of 200 kV. The nanocarrier solution (∼5 μL) was put on 400 mesh Ultrathin Type-A TEM Grid (Ted Pella, Redding, CA), immediately wicked dry by KimWipes, and then imaged directly under TEM.

Preparation of Lilial-Modified Chitosan. After chitosan (0.322 g, 2 mmol repeating unit) was completely dissolved in 30 mL of [BMIM]Cl at 90 °C, Lilial (1.225 g, 6 mmol) was added with 5 mL of DMF. After stirring for 24 h, the mixture was cooled to room temperature and poured into 200 mL of acetonitrile. The precipitation was filtered, purified completely by Soxhlet's extraction with ethanol, and finally dried in vacuum oven at 40 °C to give a yellow powder (0.633 g, 95% yield). The percentage of Lilial conjugation x (i.e., the fraction of $-NH_2$ moiety on individual CS repeating units used for Lilial conjugation) was inferred by ^{1}H NMR according to the integrated area of the characteristic peaks of Lilial (A_{Lilial}, i.e., peak *a* in Figure 1A) and CS (A_{CS}) as follows: $(4x\cdot 95.2\%)/\{[9+2(1-x)]\times 95.2\% + (9+4)\times(1-95.2\%)\} = A_{Lilial}/A_{CS}$, where 95.2% is the degree of deacetylation in CS. On the basis of the percentage of Lilial conjugation (x), the weight of Lilial (W_{Lilial}) and CS (W_{CS}) in the conjugated graft copolymer was calculated, and the Lilial loading efficiency (LE, in wt %) was estimated as $LE = W_{Lilial}/(W_{Lilial} + W_{CS}) \times 100\%$.

dx.doi.org/10.1021/ma102568p |*Macromolecules* 2011, 44, 1298–1302

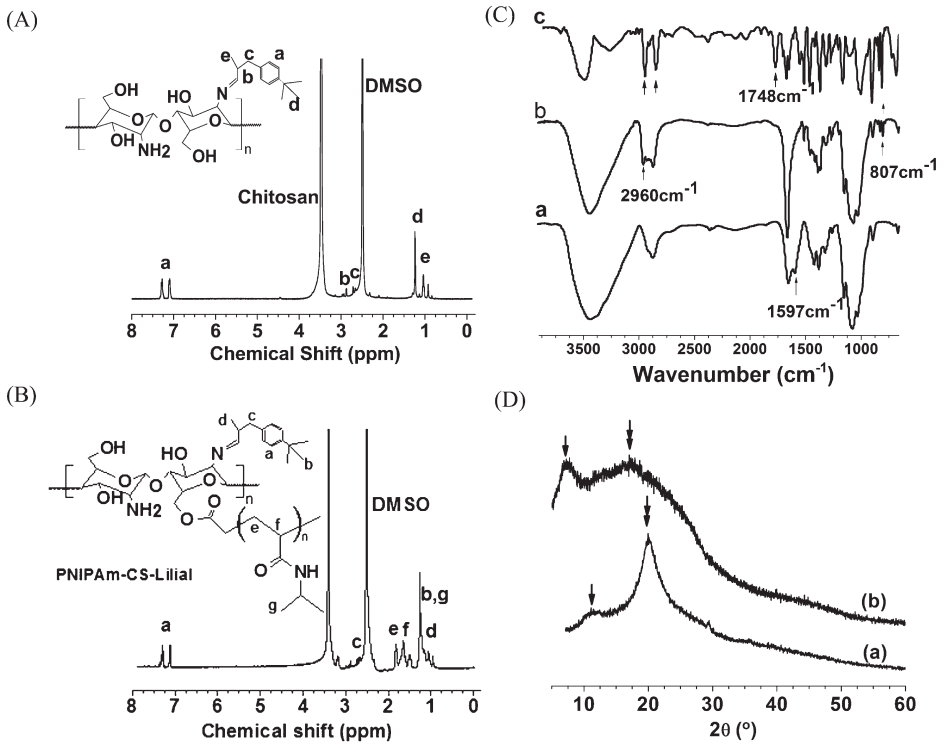

Figure 1. ^{1}H NMR spectra of (A) CS−Lilial and (B) PNIPAm−CS−Lilial (G% = 154.2%) (DMSO-d_6 as solvent, 300 MHz). (C) FT-IR spectra of (a) CS, (b) CS−Lilial, and (c) PNIPAM−CS−Lilial (graft content = 154.2%). (D) X-ray diffractions of (a) CS and (b) PNIPAm−CS−Lilial (graft content = 154.2%).

Synthesis of PNIPAm−CS−Lilial. CS−Lilial conjugate (0.347 g, 1.0 mmol repeating unit) was dissolved in dry DMF (30 mL) and reacted with prescribed amounts of carboxyl-terminated PNIPAM in the presence of DCC (0.205 g, 1.0 mmol) and DMAP (0.015 g, 0.12 mmol) for 24 h at room temperature. The resulting mixture was poured into ice water. The precipitate was collected on a filter, washed completely by Soxhlet's extraction with acetone, and dried to give a yellow powder.

The PNIPAm graft content (G%) was calculated as follows:

$$G\% = (W_g - W_0)/W_0 \times 100\%$$

where W_0 and W_g are weights of CS−Lilial before and after grafting with PNIPAm, respectively. The graft content as a function of PNIPAM/CS−Lilial (w/w) feed ratio is listed in the Supporting Information.

Self-Assembly of the Conjugated Graft Copolymer in Distilled Water. The self-assembly experiments were performed as below: a solution of graft copolymer (20 mg) in DMF (5 mL) was dialyzed (MWCO = 12K) with distilled water at room temperature. In order to remove DMF completely, the dialysis was run for 3 days and the distilled water was changed every 5 h in this period.

Release of Lilial from the Conjugated Graft Copolymer Nanocarriers. A calibration curve for Lilial quantification was obtained by measuring the absorption (λ_{max} = 264.4 nm) of a series of Lilial−hexane solution with known concentrations (absorbance A = 448c + 0.062, c (mol/L)). Lilial release profiles were determined as follows: 2 mL of PNIPAm−CS−Lilial nanocarrier solution (4 mg/mL) with a known Lilial loading efficiency was put into dialysis bag (MWCO = 12K), and each of them was immersed into 200 mL of prescribed buffers including 20% hexane. Commercial buffers at different pH were used (potassium hydrogen phthalate buffer, pH = 4.5; and 1× PBS buffers, pH = 7.4). At a definite time interval, 5 mL of hexane outside the dialysis bag was sampled, and then 5 mL of the pure hexane was infused the upper system. The Lilial concentration at time i (C^i_{Lilial}, in mol/L) was determined by UV−vis measurement according to the calibration curve. The Lilial release (%) at time i was calculated as $M_{Lilial}(VC^i_{Lilial} + \sum_{j=1}^{i-1} v_j C^j_{Lilial})/W_{Lilial}$, where M_{Lilial} is molecular weight of Lilial, W_{Lilial} is the weight of Lilial loaded into the tested nanocarriers initially, and V, v_j are the volume of hexane in the buffer solution and sampled solution (at time j), respectively.

3. RESULTS AND DISCUSSION

The CS−Lilial conjugate obtained in [BMIM]Cl has good solubility in common organic solvents such as DMF and can be directly modified to bear additional functionalities. As an example, we further graft the carboxyl-terminated PNIPAm to the CS−Lilial conjugate via a facile esterification step (Scheme 1). The PNIPAm is synthesized via a RAFT polymerization process and is carboxyl-terminated due to the use of DATC as the chain transfer agent (Supporting Information).[34,36] The PNIPAm graft content (G%) is conveniently controlled by PNIPAM/CS−Lilial (w/w) feed ratios in the esterification reaction (Supporting Information).

The CS−Lilial and PNIPAm−CS−Lilial conjugated copolymer are confirmed by ^{1}H NMR spectra (Figure 1A,B). The percentage of Lilial conjugation is also determined based on the integrated area of the characteristic peaks of Lilial and CS in the ^{1}H NMR spectrum, and it turns out 42.3% of the $-NH_2$ groups on CS have been transformed into conjugated Schiff bonds to carry Lilial molecules; i.e., the drug loading efficiency approaches 35.8 wt %. FT-IR spectra of CS, CS−Lilial, and PNIPAM−CS−Lilial (G% = 154.2%) are shown in Figure 1C as trace a, b, and c, respectively. It can be clearly seen that CS characteristic peaks at 1597 cm^{-1} ($-NH_2$) disappeared, while 807 cm^{-1} (phenyl ring) and 2960 cm^{-1} ($-CH_3$) peaks appeared for

dx.doi.org/10.1021/ma102568p |Macromolecules 2011, 44, 1298–1302

CS−Lilial (Figure 1C, trace b), indicating successful conjugation of Lilial via Schiff base bonds. After grafting with PNIPAM (Figure 1C, trace c), the characteristic peak (C═O) occurred at 1748 cm^{-1}, and the characteristic peaks at 2800−3000 cm^{-1} for $-CH_3$ were markedly enhanced. X-ray powder diffraction studies of CS before conjugation reveal its characteristic peaks at 2θ ~11° and 20° (marked by single arrow and double arrows, respectively) arising for its orthorhombic crystalline structure (Figure 1D, trace a),[37] which shift toward lower angles with a much reduced intensity after conjugation with Lilial and PNIPAm (Figure 1D, trace b). This result indicates increased lattice spacing (due to conjugation with Lilial) and a remarkably reduced CS percentage of crystalline (due to conjugation with immiscible PNIPAm), and further demonstrates that the PNIPAm−CS−Lilial conjugated copolymer was successfully synthesized by this method.

The PNIPAm−CS−Lilial conjugated copolymer self-assembles in water into core−shell nanocarriers at room temperature and neutral pH (7.4), where the water-insoluble CS−Lilial segments collapse as the cores, and the water-soluble PNIPAm segments form the corona shell. The nanocarriers have a size distribution that falls into the desired range for intravenous administration ($d \sim 142 \pm 60$ nm) as measured by TEM and DLS (Figure 2A,D). High-resolution TEM studies indicate that each nanocarrier has a diffusive boundary outside its solid core, revealing the hydrophilic PNIPAm corona structure (Figure2A, inset). Interestingly, when temperature is raised to 37 °C at this pH, the diffusive PNIPAm corona collapses on the core surface, probably forming a protective layer, and the TEM picture reveals a clear boundary edge outside the solid core (Figure 2B and inset). The predominant size of the nanocarriers is only slightly reduced ($d \sim 135 \pm 60$ nm) above the transition temperature as revealed by DLS (Figure 2D,E). These results suggest nearly intact nanocarrier size distributions and drug encapsulation during the storage and transit stage.

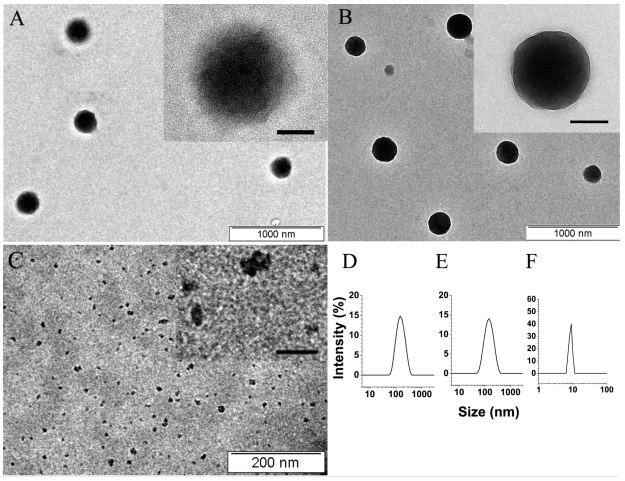

Figure 2. TEM images of self-assembled PNIPAm−CS−Lilial nanocarriers (PNIPAm graft content = 154.2%) in dilute H_2O dispersion (0.2 mg/mL) at (A) pH = 7.4 and 25 °C, (B) pH = 7.4 and 37 °C, and (C) pH = 4.5 and 37 °C (for 3 days). Scale bar: 1000 nm (A, B) and 200 nm (C). Individual nanocarriers at higher magnification are shown as the inset in (A), (B), and (C) (scale bar: 100 nm for (A) and (B); 20 nm for (C)). The nanocarrier size distributions under different conditions are measured by DLS and shown in (D) pH = 7.4 and 25 °C; (E) pH = 7.4 and 37 °C; and (F) pH = 4.5 and 37 °C (for 3 days).

Under the conditions of both enhanced temperature and acidity (T = 37 °C, pH = 4.5) mimicking endosomal or lysosomal uptake, the core−shell structure is expected to be reversed and fallen apart, e.g., PNIPAm segments become hydrophobic and collapse to form the core, whereas CS segments will be exposed as the shell, and the CS−Lilial Schiff bonds will be subjected to degradation to release Lilial molecules. TEM studies confirm the stimuli-responsive transition—the nanocarriers break apart to form reversed core−shell nanoparticles with a favorable size distribution ($d \sim 8 \pm 3$ nm) to be easily removed by renal filtration (Figure 2C,F).

To examine the time- and dose-specific release profile of Lilial before and after cellular uptake of the nanocarriers, we incubate self-assembled nanocarriers in buffers at different temperatures and pH. The percentage of Lilial release from the nanocarriers is monitored as a function of time and shown in Figure 3A. Zero release of Lilial is observed under conditions mimicking storage and transit stage in a 72 h period at neutral pH (trace a) when Lilial is encapsulated inside an insoluble CS core. In contrast to that, Lilial is released at a remarkably enhanced pace under conditions mimicking endosomal or lysosomal uptake (pH = 4.5 at 37 °C), and 70% Lilial molecules are liberated within a 30 h period (trace b). This rapid release phase is due to the fact that the core−shell nanocarriers (Figure 2 A,B) are reversed under this condition (Figure 2C), and the Lilial−conjugated CS chains are exposed to acid degradation. After the initial rapid release phase (t > 30 h), the release profile gradually plateaus with

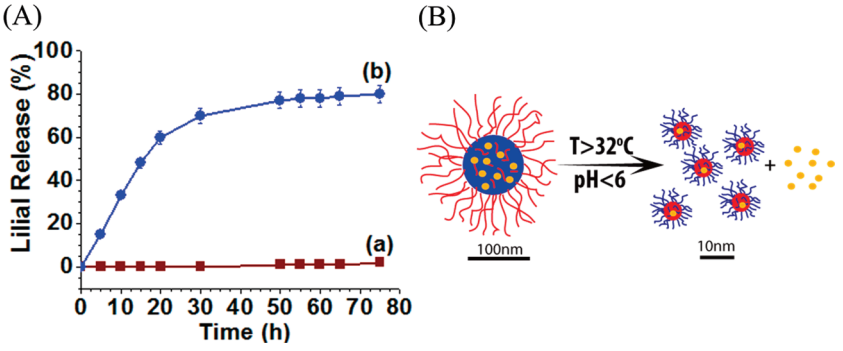

Figure 3. (A) Lilial release profile at simulated storage stage (a) and endosomal/lysosomal uptake stage (b): (a) 25 °C, pH = 7.4; (b) 37 °C, pH = 4.5. (B) Schematic representation of the dual responsive behavior of self-assembled PNIPAm−CS−Lilial nanocarriers. The PNIPAm and CS are represented in red and blue, respectively. Lilial is represented in yellow.

prolonged Lilial release at a much slower pace. The continued slow Lilial release is contributed from the acid digestion of CS−Lilial conjugated chain segments that are buried inside the PNIPAm cores during the transition, which will gradually become exposed to the surface of PNIPAm cores due to its immiscibility with PNIPAm and constant polymer chain movement. This unique stimuli-responsive behavior is schematically represented in Figure 3B: The core−corona structured nanocarriers ($d \sim 135 \pm 60$ nm) are stable under the condition of storage/transport but are reversed and broken apart as small nanoparticles ($d \sim 8 \pm 3$ nm) in response to the conditions of endosomal/lysosomal uptake to release hydrophobic payloads via cleavage of Schiff base bonds in a controlled manner: a rapid release of Lilial conjugated with the corona-forming CS occurs within a short time window ($t < 30$ h), whereas a prolonged release of Lilial at a slower pace continues as the Lilial−conjugated CS segments initially buried within PNIPAm cores gradually move to the surface of the cores.

4. CONCLUSIONS

In summary, we demonstrate a novel strategy to conjugate hydrophobic drug molecules with biocompatible and biodegradable CS via a green chemistry approach. The conjugation not only solves the intractability problem of CS and opens new avenues for CS modifications, but also is labile to stimuli-responsive cleavage. We show here as an example that thermally responsive PNIPAm can be grafted to the Lilial-conjugated CS via a facile esterification process (the ester bond itself is also biodegradable[4,10]), and the PNIPAm−CS−Lilial copolymer conjugate self-assembles into nanocarriers with a favorable size distribution and smart stimuli-responsive drug release profiles that are highly desired for intravenous administration. A similar concept should be applicable to the delivery of other hydrophobic payloads such as chemotherapy agents[31] with alternative choices of CS modification approaches if needed (for instance, grafting CS−pharmaceutical conjugates with poly(ethylene glycol) to improve circulation time[4−13]). Beyond drug delivery system design, the green chemistry approach of Schiff base bond protection−deprotection may also be extended as an easy and gentle strategy to circumvent the intractability of CS for its regioselective modification that is needed in other biomedical applications.[18,25]

■ ASSOCIATED CONTENT

Supporting Information. Synthesis and characterization of ionic liquid [BMIM]Cl and carboxyl-terminated PNIPAm; control of PNIPAm grafting content on CS. This material is available free of charge via the Internet at http://pubs.acs.org.

■ AUTHOR INFORMATION

Corresponding Author

*D.H.: Tel (+) 86-512-65882050, Fax (+) 86-512-65880089, e-mail dbhua_lab@suda.edu.cn; H.L.: Tel (+)1-303-384-2339, Fax: (+) 1-303-273-3795, e-mail hjliang@mines.edu.

■ ACKNOWLEDGMENT

This work is supported by the CSM startup fund (H.L.), Natural Science Foundation of China (50903060), Specialized Research Fund for the Doctoral Program of Higher Education of China (20093201120004), and Program of Innovative Research Team of Soochow University. We thank Dr. Byung-Tae Lee from Prof. James Ranville's group at CSM for his help with DLS measurements.

■ REFERENCES

(1) Lacko, A. G.; Nair, M.; Prokai, L.; McConathy, W. J. *Expert Opin. Drug Delivery* **2007**, *4*, 665–675.
(2) van Vlerken, L. E.; Vyas, T. K.; Amiji, M. M. *Pharm. Res.* **2007**, *24*, 1405–1414.
(3) Fox, M. E.; Szoka, F. C.; Frechet, J. M. J. *Acc. Chem. Res.* **2009**, *42*, 1141–1151.
(4) Duncan, R. *Nat. Rev. Cancer* **2006**, *6*, 688–701.
(5) Duncan, R. *Biochem. Soc. Trans.* **2007**, *35*, 56–60.
(6) Tong, R.; Cheng, J. J. *Polym. Rev.* **2007**, *47*, 345–381.
(7) Khemtong, C.; Kessinger, C. W.; Gao, J. M. *Chem. Commun.* **2009**, 3497–3510.
(8) Park, J. H.; Lee, S.; Kim, J. H.; Park, K.; Kim, K.; Kwon, I. C. *Prog. Polym. Sci.* **2008**, *33*, 113–137.
(9) Parveen, S.; Sahoo, S. K. *J. Drug Targeting* **2008**, *16*, 108–123.
(10) Uhrich, K. E.; Cannizzaro, S. M.; Langer, R. S.; Shakesheff, K. M. *Chem. Rev.* **1999**, *99*, 3181–3198.
(11) Hillaireau, H.; Couvreur, P. *Cell. Mol. Life Sci.* **2009**, *66*, 2873–2896.
(12) Kim, D. K.; Dobson, J. *J. Mater. Chem.* **2009**, *19*, 6294–6307.
(13) Choi, H. S.; Liu, W.; Misra, P.; Tanaka, E.; Zimmer, J. P.; Ipe, B. I.; Bawendi, M. G.; Frangioni, J. V. *Nature Biotechnol.* **2007**, *25*, 1165–1170.
(14) Kumar, M.; Muzzarelli, R. A. A.; Muzzarelli, C.; Sashiwa, H.; Domb, A. J. *Chem. Rev.* **2004**, *104*, 6017–6084.
(15) Pillai, C. K. S.; Paul, W.; Sharma, C. P. *Prog. Polym. Sci.* **2009**, *34*, 641–678.
(16) Kean, T.; Thanou, M. *Adv. Drug Delivery Rev.* **2010**, *62*, 3–11.
(17) Agnihotri, S. A.; Mallikarjuna, N. N.; Aminabhavi, T. M. *J. Controlled Release* **2004**, *100*, 5–28.
(18) Carreira, A. S.; Goncalves, F.; Mendonca, P. V.; Gil, M. H.; Coelho, J. F. J. *Carbohydr. Polym.* **2010**, *80*, 618–630.
(19) Ravindra, R.; Krovvidi, K. R.; Khan, A. A. *Carbohydr. Polym.* **1998**, *36*, 121–127.
(20) Erbacher, P.; Zou, S. M.; Bettinger, T.; Steffan, A. M.; Remy, J. S. *Pharm. Res.* **1998**, *15*, 1332–1339.
(21) de la Fuente, M.; Ravina, M.; Paolicelli, P.; Sanchez, A.; Seijo, B.; Alonso, M. J. *Adv. Drug Delivery Rev.* **2010**, *62*, 100–117.
(22) Banerjee, T.; Mitra, S.; Singh, A. K.; Sharma, R. K.; Maitra, A. *Int. J. Pharm.* **2002**, *243*, 93–105.
(23) Andersson, M.; Lofroth, J. E. *Int. J. Pharm.* **2003**, *257*, 305–309.
(24) Kurita, K.; Ikeda, H.; Yoshida, Y.; Shimojoh, M.; Harata, M. *Biomacromolecules* **2002**, *3*, 1–4.
(25) Makuska, R.; Gorochovceva, N. *Carbohydr. Polym.* **2006**, *64*, 319–327.
(26) Kratz, F.; Beyer, U.; Schutte, M. T. *Crit. Rev. Ther. Drug Carrier Syst.* **1999**, *16*, 245–288.
(27) Charles, A. K.; Darbre, P. D. *J. Appl. Toxicol.* **2009**, *29*, 422–434.
(28) Rogers, R. D.; Seddon, K. R. *Science* **2003**, *302*, 792–793.
(29) Xie, H. B.; Zhang, S. B.; Li, S. H. *Green Chem.* **2006**, *8*, 630–633.
(30) Pisco, L.; Kordian, M.; Peseke, K.; Feist, H.; Michalik, D.; Estrada, E.; Carvalho, J.; Hamilton, G.; Rando, D.; Quincoces, J. *Eur. J. Med. Chem.* **2006**, *41*, 401–407.
(31) Wang, B. D.; Xu, C. J.; Xie, J.; Yang, Z. Y.; Sun, S. L. *J. Am. Chem. Soc.* **2008**, *130*, 14436–14437.
(32) Kubota, K.; Fujishige, S.; Ando, I. *J. Phys. Chem.* **1990**, *94*, 5154–5158.
(33) Wu, C.; Zhou, S. *Macromolecules* **1995**, *28*, 8381–8387.
(34) Lai, J. T.; Filla, D.; Shea, R. *Macromolecules* **2002**, *35*, 6754–6756.
(35) Dyson, P. J.; Grossel, M. C.; Srinivasan, N.; Vine, T.; Welton, T.; Williams, D. J.; White, A. J. P.; Zigras, T. *J. Chem. Soc., Dalton Trans.* **1997**, 3465–3469.
(36) Convertine, A. J.; Ayres, N.; Scales, C. W.; Lowe, A. B.; McCormick, C. L. *Biomacromolecules* **2004**, *5*, 1177–1180.
(37) Samules, R. J. *J. Polym. Sci., Polym. Phys. Ed.* **1981**, *19*, 1081–1105.